THE JOURNAL OF BIOLOGICAL CHEMISTRY
Vol. 278, No. 42, Issue of October 17, pp. 41491–41499, 2003
Printed in U.S.A.

Structure of the Monomeric 8-kDa Dynein Light Chain and Mechanism of the Domain-swapped Dimer Assembly*

Received for publication, July 3, 2003, and in revised form, August 4, 2003
Published, JBC Papers in Press, August 6, 2003, DOI 10.1074/jbc.M307118200

Wenning Wang‡§¶, Kevin W.-H. Lo‡, Ho-Man Kan‡, Jing-Song Fan‡, and Mingjie Zhang‡‖

From the ‡Department of Biochemistry, Molecular Neuroscience Center, The Hong Kong University of Science and Technology, Clear Water Bay, Kowloon, Hong Kong, People's Republic of China and the §Department of Chemistry, Fudan University, 220 Handan Road, Shanghai, People's Republic of China

The 8-kDa light chain of dynein (DLC8) is ubiquitously expressed in various cell types. Other than serving as a light chain of the dynein complexes, this highly conserved protein has been shown to bind a larger number of proteins with diverse biological functions. DLC8 forms a homodimer via three-dimensional domain swapping of an internal β-strand (the β2-strand) at neutral pH. The protein undergoes non-reversible dimer-to-monomer dissociation when the pH value of the protein solution decreases. The three-dimensional structure of the DLC8 monomer determined by NMR spectroscopy at pH 3.0 showed that the protein is well folded. The major conformational change accompanied by dimer dissociation is in the β2-strand of the protein, which undergoes transition from a β-strand to a nascent α-helix. The monomer form of DLC8 is not capable of binding to target proteins. Insertion of two flexible amino acid residues in the tight β1/β2-loop dramatically stabilized the monomer conformation of the protein. NMR studies showed that the mutation altered the conformation as well as the three-dimensional domain swapping-mediated assembly of the DLC8 dimer. The mutant DLC8 was unable to bind to its targets even at physiological pH. The three-dimensional structure of the mutant protein in its monomeric form provides the structural basis of the mutation-induced stabilization of the monomer conformation. Based on the experimental data, we conclude that the formation of the β2-strand swapping-mediated dimer is mandatory for the structure and function of DLC8. We further note that the DLC8 dimer represents a novel mode of three-dimensional domain swapping.

Dyneins are microtubule-based molecular motors that provide forces for various motility processes in eukaryotic cells (1–4). The dynein superfamily proteins are divided into two major classes based on their distinct cellular functions. Cytoplasmic dyneins are involved in membrane-bound organelle transport, Golgi localization, spindle formation and orientation, and nuclear localization. Axonemal dyneins are largely responsible for providing motive force for ciliary and flagellar beating. All known dyneins contain multiple subunits, and the complexes have molecular masses of >1 MDa. Typically each dynein contains two or three heavy chains, each with molecular mass ~500 kDa (the globular heads of heavy chains contain ATPase activity); two or more intermediate chains (molecular mass, 70–80 kDa) that are apparently involved in attachment of the motor to some of its cargoes; and several light chains (molecular mass, 8–22 kDa) of which the precise functions are still largely unknown (1–4). Cytoplasmic dyneins also contain multiple copies of light intermediate chains that are distantly related to ABC transporters (5, 6).

The 8-kDa light chain of dynein (DLC8)[1] is the smallest subunit in the motor complex. DLC8 was originally identified as a light chain of *Chlamydomonas* outer arm axonemal dynein (7, 8). The protein was subsequently shown to be a stoichiometric component of cytoplasmic dyneins (9) and actin-based motor myosin V (10, 11). DLC8 exists as a dimer under physiological conditions (10). Cellular fractionation of mammalian brain extracts revealed that only a minor fraction of DLC8 exists as a dynein-bound form, and the majority of the protein is not associated with microtubules (9). The extremely high amino acid sequence conservation throughout evolution and the existence of multiple pools of the protein suggest that DLC8 may be involved in conserved functions in various biological processes. Indeed a growing number of proteins have been identified to interact with DLC8, and these DLC8-binding proteins are apparently involved in diverse biological processes. For example, DLC8 was found to specifically interact with neuronal nitric-oxide synthase (12, 13), proapoptotic Bcl-2 family protein Bim and Bmf (14, 15), mRNA localization protein Swallow (16), and postsynaptic scaffold proteins GKAP and gephyrin (17, 18). Structural studies showed that the DLC8 dimer contains two symmetric target-binding channels (19, 20). DLC8-binding domains are confined to a short stretch of continuous peptide fragment of less than 15 amino acid residues (13, 21, 22). Upon complex formation, a DLC8-bound peptide assumes a β-strand structure and augments the antiparallel β-sheet of DLC8 by pairing with the β2-strand of the protein (19, 20). In *Drosophila*, partial mutation of DLC8 gene leads to defects in fly's bristle and wing development, female sterility, and abnormal sensory axon projections; total loss-of-function mutations are lethal due to apoptosis (23, 24). Mutation of DLC8 in *Aspergillus nidulans* inhibits nuclear migration (25). Disruption of the

* This work was supported by Grants HKUST6207/00M, HKUST6097/01M, HKUST6125/02M, and AOE/B15/01 from the Research Grant Council of Hong Kong, a Philip Morris Inc. external research grant (to M. Z.), and National Natural Science Foundation of China Grant 20103002 (to W. W.). The costs of publication of this article were defrayed in part by the payment of page charges. This article must therefore be hereby marked "*advertisement*" in accordance with 18 U.S.C. Section 1734 solely to indicate this fact.

The atomic coordinates and structure factors (code IPWJ and 1PWK) have been deposited in the Protein Data Bank, Research Collaboratory for Structural Bioinformatics, Rutgers University, New Brunswick, NJ (http://www.rcsb.org/).

¶ A visiting professor sponsored by the Croucher Foundation.

‖ A senior research fellow of the Croucher Foundation. To whom correspondence should be addressed. Tel.: 852-2358-8709; Fax: 852-2358-1552; E-mail: mzhang@ust.hk.

[1] The abbreviations used are: DLC8, 8-kDa light chain of dynein; HSQC, heteronuclear single quantum correlation; GST, glutathione *S*-transferase; NOE, nuclear Overhauser effect; NOESY, NOE spectroscopy; TOSCY, total correlation spectroscopy; r.m.s., root mean square.

interaction between DLC8 and Swallow destroys the asymmetric distribution of Swallow (16). DLC8 functions as a regulator of apoptosis by sequestering the proapoptotic proteins Bim and Bmf on cytoskeletal structures via dynein and myosin V complexes (14, 15).

Mammalian cells contain two 8-kDa light chains, and these two light chains are encoded by two different genes (17, 24). However, the two gene products share extremely high sequence identity (83 of a total of 89 residues are identical). Among six different amino acid residues, only three are not homologous replacement. The three non-homologous residues are located in the unstructured N terminus (residue 2) and solvent-exposed α-helices (residues 21 and 41). Both of the light chains appear to be able to interact with dynein and myosin V motors as well as known DLC8-binding proteins. The functional significance of having the two light chains is still unknown. For nomenclature consistency, DLC8 (also called PIN, DLC1, and LC1) is named as DLC8a, and the other light chain (also called LC2) is referred as DLC8b throughout this study. We use DLC8 to refer to both light chains.

In this work, we studied the pH-dependent dimer-monomer equilibrium of DLC8b. The structure of DLC8b in its monomeric form was determined by NMR spectroscopy. We further addressed structural and functional basis of the three-dimensional domain swapping-mediated DLC8 dimer assembly. We chose to use DLC8b, instead of DLC8a, as the monomeric form of DLC8b is more stable and amenable for detailed NMR structural characterization.

MATERIALS AND METHODS

Sample Preparation—The recombinant rat DLC8b was expressed, purified, and isotope-labeled with essentially identical methods as those described in our previous studies of DLC8a (20, 26). The mutants of DLC8b used in this study were generated by standard PCR-based techniques.

All NMR samples were dissolved in 90% H_2O, 10% D_2O or 99.99% D_2O. To obtain pure monomeric DLC8b, the sample pH was adjusted to 3.0. The concentrations of the DLC8b monomer of the NMR samples for structural determination were ~1.0 mM. The concentrations of the NMR samples for ^1H,^{15}N HSQC-based pH titrations and target peptide binding experiments were in the range of 0.3–0.5 mM.

Pull-down Binding Assay—Direct interaction between DLC8b and GST-fused proteins were assayed in the phosphate-buffered saline (pH 7.5). An equal molar amount of DLC8 and one of the GST fusion proteins (0.6 nmol each) were mixed in 100 μl of the assay buffer. The GST fusion protein-DLC8b complexes were pelleted by 30 μl of a slurry of GSH-Sepharose beads. The pellets were washed three times with 0.5 ml of the assay buffer and subsequently boiled with 30 μl of 2× SDS-PAGE sample buffer. The intensity of the DLC8b band on SDS-polyacrylamide gels was used to judge the strength of the interaction between DLC8b and its target proteins.

Analytical Gel Filtration Chromatography—The molecular masses of various forms of DLC8b at different pH values were determined by analytical gel filtration chromatography using a Superose 12 column (Amersham Biosciences).

NMR Spectroscopy—All NMR experiments were carried out at 30 °C on Varian Inova 500 and 750 MHz spectrometers. NMR spectra were processed with the NMRpipe software package (27) and analyzed with PIPP (28) and Sparky. Sequential backbone resonance assignment of the DLC8b monomer was obtained by standard heteronuclear correlation experiments including HNCACB, CBCA(CO)NH, and HNCO and confirmed by a three-dimensional ^{15}N-separated NOESY experiment (29–31). The non-aromatic non-exchangeable side chain assignments were obtained using an HCCH-TOCSY experiment. The side chains of the aromatics were assigned by ^1H two-dimensional TOCSY and NOESY experiments with an unlabeled DLC8b sample in D_2O (32).

Structural Calculation—The interproton distance restraints were derived from NOESY spectra (a ^1H two-dimensional homonuclear NOESY, a ^{15}N-separated NOESY, and a ^{13}C-separated NOESY for the wild type DLC8b). NOEs were grouped into three distance ranges: 1.8–2.7 Å (1.8–2.9 Å for NOEs involving HN protons), 1.8–3.3 Å (1.8–3.5 Å for NOEs involving HN protons), and 1.8–5.0 Å, corresponding to strong, medium, and weak NOEs. Hydrogen bond restraints (two per hydrogen bond where $r_{NH\text{-}O}$ = 1.8–2.2 Å and $r_{N\text{-}O}$ = 2.2–3.3 Å) were generated by a combination of the standard secondary structure of the protein based on NOE patterns and backbone secondary chemical shifts. Backbone dihedral angle restraints (ϕ and ψ angles) were derived from the backbone chemical shift analysis program TALOS (33). Structures were calculated using the program CNS (34). The calculated structures were assessed with PROCHECK-NMR (35). The figures were generated using MOLMOL (36), MOLSCRIPT (37), Raster3D (38), and GRASP (39).

Protein Data Bank Coordinates—The coordinates of the DLC8b monomer and the DLC8bInsSG monomer structures have been deposited in the Research Collaboratory for Structural Bioinformatics Protein Data Bank (accession code 1PWJ and 1PWK, respectively) with the designation of immediate release upon publication (HPUB).

RESULTS

pH-dependent Dissociation of DLC8b—It has been well characterized that DLC8a exists as a homodimer at the physiological pH, and the two monomers of DLC8a form a domain-swapped dimer by exchanging the β2-strands (19, 20). Due to the extreme high amino acid homology between the two dynein light chains, DLC8b exists as a dimer with the structure nearly identical to that of DLC8a at pH 7.0 (data not shown). Similar to what was observed in DLC8a (19, 20, 40), DLC8b also displays a pH-dependent dimer-monomer equilibrium. At pH 7.0, DLC8b is entirely dimeric (Fig. 1, *A* and *B*). When the pH value of the protein solution decreases, the monomeric population of DLC8b gradually increases. At pH 3.0, the protein completely dissociates into a monomeric form (Fig. 1, *A* and *B*). Judging from the uniformity of the peak intensities and the large chemical shift dispersion of the ^1H,^{15}N HSQC spectrum of the protein at pH 3.0, we conclude that the monomeric form of DLC8b is stably folded (Fig. 1*B*). We further noted that this pH-dependent dimer-to-monomer dissociation is not reversible as the dimer peaks were never observed to reappear when the solution pH values were raised back to neutral. Fig. 2 summarizes the backbone $^{13}C_\alpha$ chemical shift differences between the dimer and the monomer forms of DLC8b. It is clear that the amino acid residues in the Arg^{60}–His^{72} region of the protein show large chemical shift differences between the two forms. The rest of the protein displays relatively small chemical shift changes when the protein dissociates from a dimer to two monomers. The chemical shift data shown in Fig. 2 indicate that the Arg^{60}–His^{72} region of DLC8b undergoes major conformational changes when the protein dissociates into the monomeric form. The rest of the protein shares the similar structure in both the dimer and the monomer forms. Since the amino acid residues that undergo prominent chemical changes (thus, the conformational changes) upon dimer dissociation are in the β2-strand of the DLC8b dimer and the β2-strand of DLC8b (as in DLC8a) is known to be responsible for target binding in its dimer form, we sought to determine whether the DLC8b monomer retains its target binding capacity.

To investigate this point, we titrated the ^{15}N-labled DLC8b monomer (pH 3.0) with several DLC8 dimer-binding peptides. A ^1H,^{15}N HSQC spectrum was recorded for each peptide/DLC8b mixture. The peptides that we used include the DLC8-binding motif of dynein intermediate chain, DLC8-binding domain of Bim, and the DLC8-binding peptide of neuronal nitric-oxide synthase (13, 21). All of these peptides were shown to bind to the DLC8b dimer in a fashion similar to that previously reported for the DLC8a dimer (data not shown). In contrast, none of these peptides were able to interact with the DLC8b monomer based on our NMR experiment as the HSQC spectrum of the DLC8b monomer showed no observable chemical shift changes upon the addition of these peptides (data not shown).

Overall Structure of the DLC8b Monomer—To obtain a definitive picture of the conformational changes of DLC8b upon

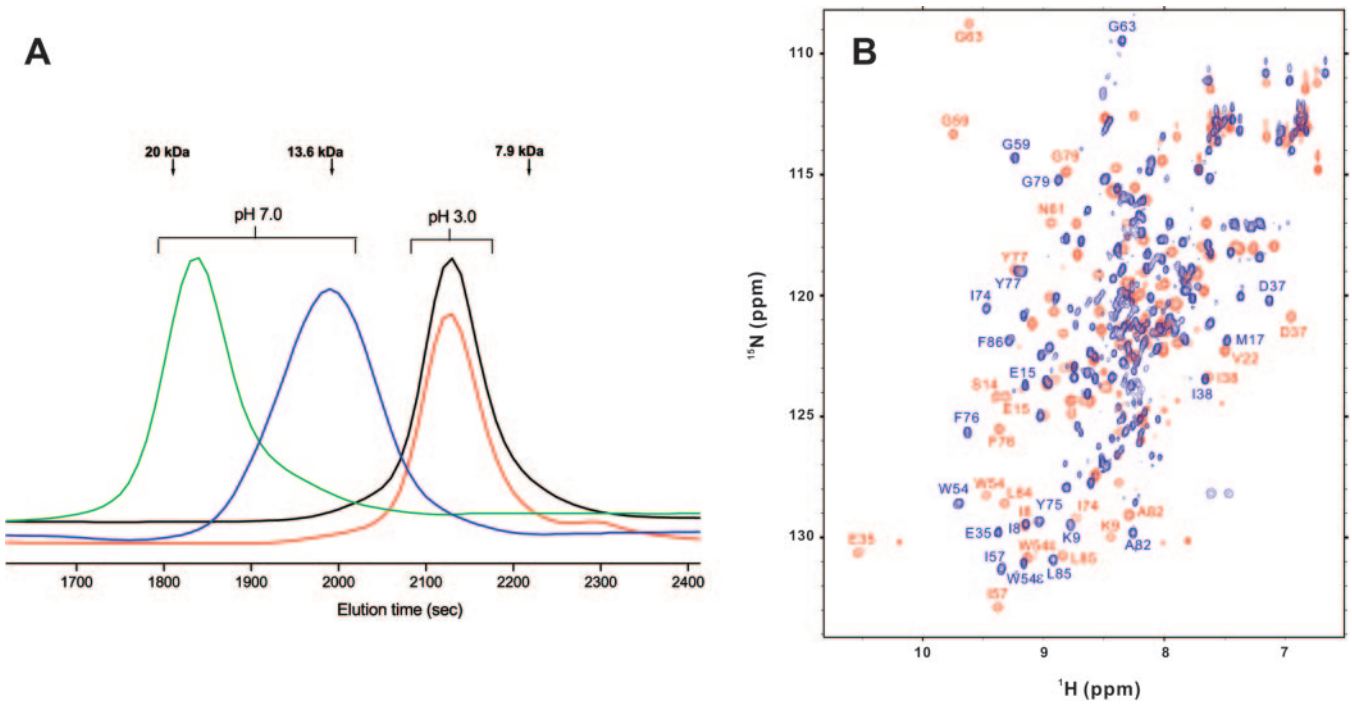

FIG. 1. **pH-dependent dimer-monomer equilibrium of DLC8b.** *A*, analytical gel filtration chromatography elution profiles of DLC8b and DLC8bInsSG at pH 7.0 and 3.0. The elution curves of DLC8b at pH 7.0 and 3.0 are shown in *green* and *black*, respectively. The elution profiles of DLC8bInsSG at pH 7.0 and 3.0 are in *blue* and *red*, respectively. The elution times of the protein markers used to calibrate the gel filtration column are labeled at the *top* of the figure. *B*, superposition of the ^{1}H,^{15}N HSQC spectra of ^{15}N-labeled DLC8b at pH 7.0 (*red*) and 3.0 (*blue*). The assignments of selected amino acid residues of the protein at both pH values are labeled.

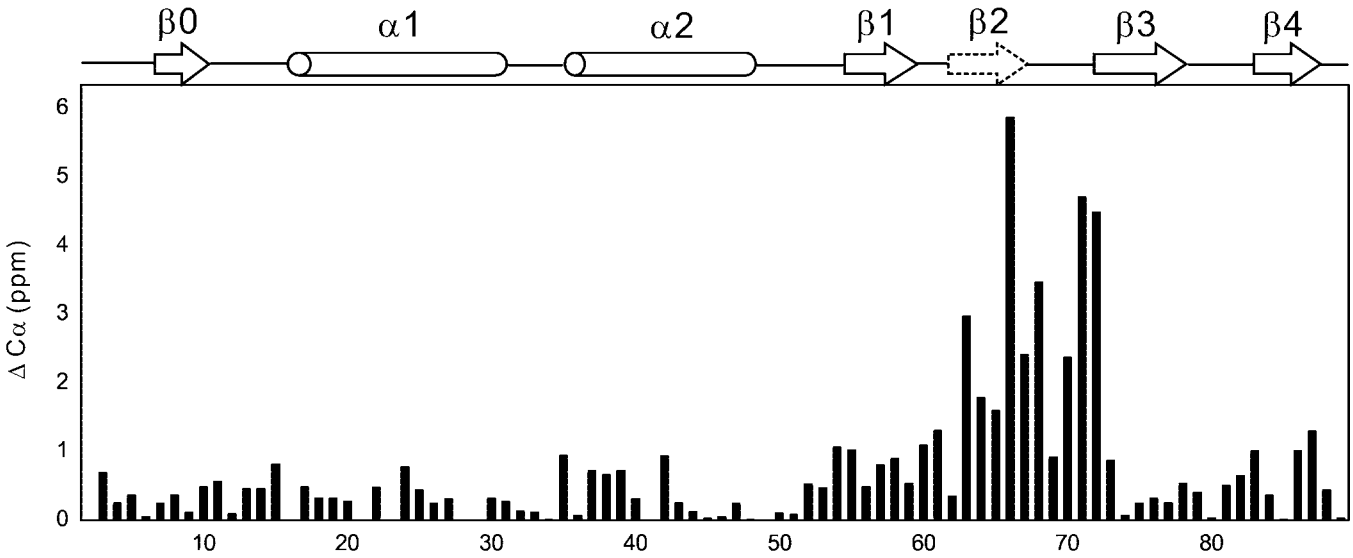

FIG. 2. **Plot of the $^{13}C_{\alpha}$ chemical shift differences as a function of amino acid residue number of DLC8b at pH 7.0 and 3.0.** The $^{13}C_{\alpha}$ chemical shift differences were expressed as the absolute value for each amino acid residue. The secondary structure of DLC8b in its dimer form is shown at the *top* of the figure. The β2-strand is drawn as a *dashed arrow* to highlight the conformational differences of this region at the two pH values.

the dimer dissociation, we decided to determine the three-dimensional structure of DLC8b monomer at pH 3.0 using standard multidimensional NMR spectroscopic techniques. We chose DLC8b, instead of DLC8a, due to the superb stability of DLC8b monomer (pH 3.0) at concentrations suitable for NMR structural determination. At pH 3.0, DLC8a does not completely dissociate into monomer. Further decreases in solution pH lead to partial denaturation and precipitation of DLC8a (data not shown). A total of 1,852 experimental restraints were used to calculate the solution structure of the DLC8b monomer (Table I). Fig. 3*A* shows the superposition of the final 20 simulated annealing structures of DLC8b, and Fig. 3*B* shows a ribbon diagram representation of the DLC8b monomer. For the convenience of structural comparison, we use the same nomenclature for the secondary structure elements of the DLC8b monomer as that used for the DLC8a dimer (20). Except for the N-terminal four residues and the amino acids 61–71 (the β2-strand and the β2/β3-loop in the DLC8 dimer), the structure of the rest of DLC8b monomer is well defined (Fig. 3*A*). The DLC8b monomer contains two α-helices (α1 and α2) and four β-strands (β0, β1, β3, and β4). The four β-strands forms an antiparallel β-sheet with a topology of β0-β3-β4-β1. The β-sheet is sandwiched on one side by the two α-helices and on the other by a loop-like structure connecting β1 and β3 (see

TABLE I

Structural statistics for the family of 20 structures of the DLC8b and DLC8bInsSG monomer

None of the structures exhibits distance violations greater than 0.3 Å or dihedral angle violations greater than 4°.

	DLC8b	DLC8bInsSG
Distance restraints		
Intraresidue ($i - j = 0$)	621	290
Sequential ($i - j = 1$)	393	370
Medium range ($2 < i - j < 4$)	270	223
Long range ($i - j > 5$)	428	178
Hydrogen bonds	66	66
Total	1778	1129
Dihedral angle restraints		
Φ	37	37
Ψ	37	37
Total	74	74
Mean r.m.s. deviations from the experimental restraints		
Distance (Å)	0.012 ± 0.001	0.022 ± 0.001
Dihedral angle (Å)	0.021 ± 0.018	0.116 ± 0.054
Mean r.m.s. deviations from idealized covalent geometry		
Bond (Å)	0.002 ± 0.000	0.003 ± 0.000
Angle (Å)	0.380 ± 0.015	0.435 ± 0.010
Improper (Å)	0.281 ± 0.018	0.337 ± 0.014
Mean energies (kcal mol^{-1})		
E_{NOE}[a]	19.25 ± 2.62	41.19 ± 2.97
E_{cdih}[a]	0.00 ± 0.00	0.07 ± 0.07
$E_{\mathrm{L-J}}$	−194.89 ± 14.37	−124.79 ± 22.63
Ramachandran plot, secondary structure		
Percentage of residues in the most favored regions	82.0	78.8
Percentage of residues in additional allowed regions	16.0	15.4
Percentage of residues in generously allowed regions	2.0	3.8
Percentage of residues in disallowed regions	0	1.9
Atomic r.m.s. differences (Å)[b], secondary structure		
Backbone heavy atoms (N, C_α, and C′)	0.46	0.51
Heavy atoms	1.12	1.12

[a] The final values of the square-well NOE and dihedral angle potentials were calculated with force constants of 50 kcal mol^{-1} Å^{-2} and 200 kcal mol^{-1} radian^{-2}, respectively.

[b] The precision of the atomic coordinates is defined as the average r.m.s. difference between the 20 final structures and the mean coordinates of the protein.

below for more details). The DLC8b monomer adopts a globular overall structure in solution. Except for the loop connecting the β1- and β3-strands, the rest of the DLC8b monomer has a conformation remarkably similar to the corresponding segments in the dimer form of DLC8a (Fig. 3), a result that is entirely consistent with the chemical shift perturbation data shown in Fig. 2 and earlier CD and fluorescence studies (40). Structural comparison between the DLC8b monomer and a subunit of the DLC8a dimer using the two helices and the four β-strands (β0, β1, β3, and β4) gives rise to an r.m.s. deviation value of 1.38 Å (Fig. 3*C*).

Conformational Changes Accompanying Dimer Dissociation—The largest conformational changes that occur in DLC8b upon dimer dissociation are found in the β2-strand. In the dimer, the β2-strand crosses over to the neighboring subunit and forms an antiparallel β-sheet with the β1-strand within that subunit (19, 20). The corresponding amino acid residues in the DLC8b monomer do not form a stable regular secondary structure, although the whole segment protrudes from the main antiparallel β-sheet. We refer to this segment of the DLC8b monomer as the β2-loop for convenience and nomenclature consistency. NOE connectivities of the backbones of the β2-loop residues showed characteristics of a nascent α-helical structure (*i.e.* continuous medium-to-strong backbone d_{NN} and weak $d_{\alpha\mathrm{N}(i,\,i+3)}$ NOEs connectivities, data not shown). The chemical shift index data also show that the C_α/C_β chemical shifts of the residues in the β2-loop systematically shift toward an α-helical conformation, although the scale of the shift is considerably smaller than that of a stable α-helix such as α1 or α2 (Fig. 4).

In addition to the β2-loop, the amino acid residues at the end of the β1-strand and the β1/β2 linker also undergo significant conformational changes. Specifically the β1-strand is one residue shorter than that in the dimer. The shortening of the β1-strand appears to be essential for the β2-loop to form a relatively loose, nascent α-helix structure (instead of extended β-strand structure in the dimer) (19, 20). The packing of the β2-loop with the β1- and β3-strands is largely mediated by hydrophobic interactions. The formation of a nascent α-helical structure of the β2-loop appears to be essential for the stabilization of the monomer. This is because the hydrophobic face of the "helix" covers part of the otherwise solvent-exposed hydrophobic interface in the dimer, and the hydrophilic face of the helix is exposed to the solvent (Fig. 5*A*). It is worth noting that the unique non-prolyl cis-peptide bond between Pro^{52} and Thr^{53} at the α2/β1 link remains in the DLC8b monomer (20, 26). The side chain of Trp^{54} was suggested to play a critical role in stabilizing the non-prolyl cis-peptide bond in the DLC8a dimer (26). The indole ring of Trp^{54} in the DLC8b monomer occupies a position nearly identical to that seen in the DLC8a dimer (Fig. 3*C*), which explains the retention of the cis-peptide bond in the DLC8b monomer.

The β2-strand-mediated DLC8 Dimer Assembly—We next investigated the structural requirements of the β2-strand-mediated DLC8 dimer assembly and the role of the β2-strand swapping in the target binding of the protein. The β1- and β2-strands in the DLC8 dimer are linked by single amino acid residue Asn^{61} (19, 20). In this respect, we wondered whether the tight β1/β2 linker might be responsible for forcing the β2-strand to cross over to the neighboring subunit to pair with its β1-strand. In the monomer, the β1/β2 linker is too short to allow the β2-strand to swing back to form an antiparallel β-sheet with the β1-strand. To test this hypothesis, we created two DLC8b mutants by inserting one (Ser) or two (Ser-Gly) flexible amino acid residues between Arg^{60} and Asn^{61}. Both mutants with the lengthened β1/β2 linker can be expressed in

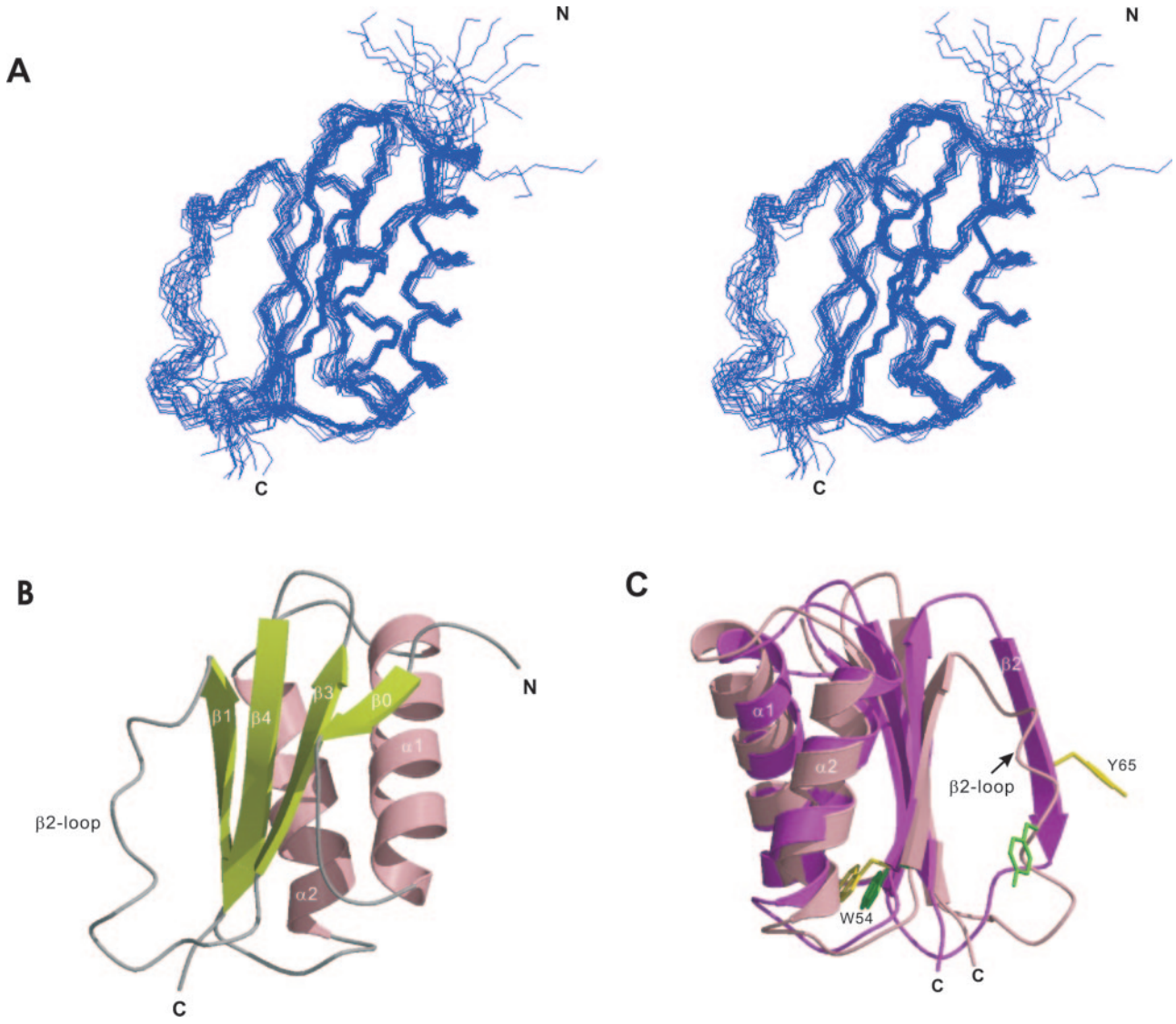

FIG. 3. **Three-dimensional structure of the DLC8b monomer.** *A*, stereoview showing the best fit superposition of the backbone atoms (N, C_α, and C′) of the final 20 structures of the DLC8b monomer. The structures are superimposed against the energy-minimized average structure using the residues adopting regular secondary structures. The N and C termini of the protein are labeled. *B*, ribbon diagram representation of the DLC8b monomer. The secondary structural elements of the protein are labeled as described previously for the dimeric protein (20). The molecule is drawn at the same orientation as shown in *A*. *C*, comparison of the three-dimensional structure of the DLC8b monomer to that of one subunit in the DLC8a dimer. The backbones of the secondary structured regions (β0, β1, β3, β4, α1, and α2) of the DLC8b monomer (*pale pink*) and a subunit of the DLC8a dimer (*magenta*) are superimposed to each other. The side chains of Trp^{54} and Tyr^{65} in the both structures are drawn using explicit atom representations.

and purified from bacterial cells in large quantities. The elution profiles obtained from analytical gel filtration chromatography showed that both mutants displayed pH-dependent elution volume changes (Fig. 1*A*). The mutant with the "Ser-Gly" insertion into the β1/β2 linker (termed as "DLC8bInsSG") showed significant elution volume as well as peak shape changes at pH 7.0 when compared with the wild type protein (Fig. 1*A*). Both the increased elution volume and broadened elution peak suggests that the mutation leads to an equilibrium between multiple conformers. At pH 3.0, the mutant was eluted as a monomer indistinguishable from that of the wild type protein. We further tested the target binding ability of this DLC8b mutant using pull-down assays. We found that DLC8bInsSG was unable to bind to various classes of DLC8 targets at both pH 7.5 and 3.0 (Fig. 6).

We next performed a detailed structural characterization of DLC8bInsSG since this mutant was completely lacking target binding capabilities at both pH 7.5 and 3.0. The number of peaks in the $^{1}H,^{15}N$ HSQC spectrum of the mutant at pH 7.0 is significantly larger than a single set of resonances seen in the wild type protein (87 observable backbone amide resonances, Fig. 1*B*), consistent with the gel filtration observation that the mutant is not a pure dimer at neutral pH. Upon gradual decreasing of the sample pH values, one set of peaks (Fig. 7, *red* peaks) experienced little chemical shift changes, and another set of resonances showed pH-dependent intensity decrease and eventual disappearance (Fig. 7, *green* peaks). At pH 3.0, we observed a single set of backbone amide resonances in the HSQC spectrum of the mutant, corresponding to the monomer conformation of the protein (Fig. 7, *red* peaks). At pH 8.5, the resonances corresponding to the monomer form of the protein almost completely disappeared, and the other set of the peaks dominated the spectrum (data not shown). We attribute the remaining set of the resonances to the dimer form of the protein as the gel filtration experiment showed that the protein has a molecular mass between dimer and monomer at pH 7.0 (Fig. 1*A*). Taken together, the NMR-based pH titration experiment showed that the DLC8bInsSG mutant establishes a dimer-

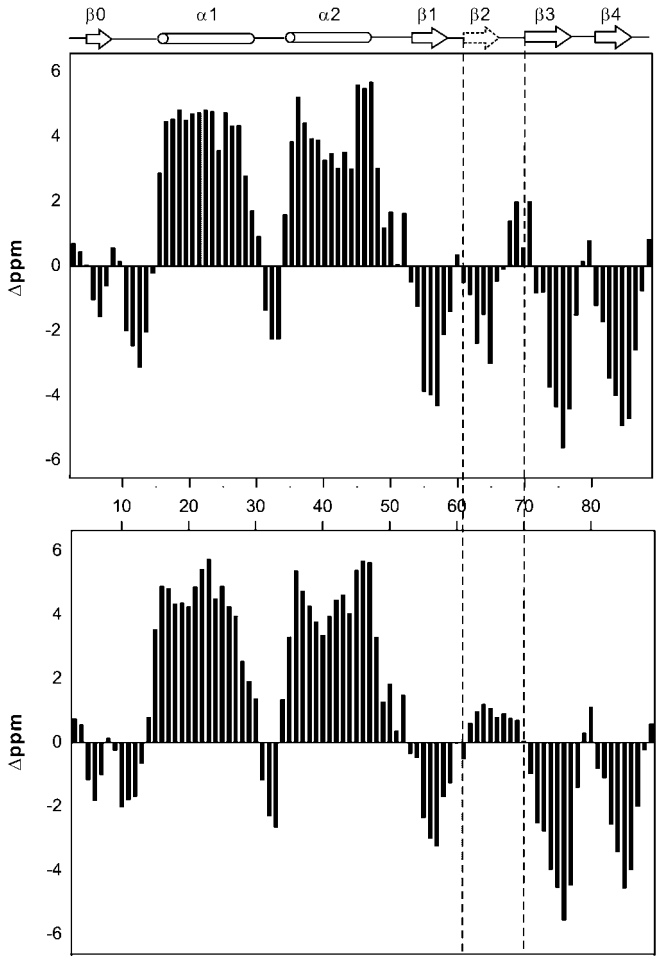

FIG. 4. **The secondary structure of the monomeric and dimeric DLC8b.** The figure shows combined C_α/C_β chemical shift index plots of the DLC8b dimer (*A*) and monomer (*B*). The combined secondary chemical shift (Δppm) for each residue is defined as Δppm = $(^{13}C_{\alpha,exp} - {}^{13}C_{\alpha,rc}) - (^{13}C_{\beta,exp} - {}^{13}C_{\beta,rc})$ where $^{13}C_{\alpha,exp}$ and $^{13}C_{\beta,exp}$ are experimental chemical shifts of $^{13}C_\alpha$ and $^{13}C_\beta$, respectively, and $^{13}C_{\alpha,rc}$ and $^{13}C_{\beta,rc}$ are random coil chemical shifts for each residue. Each data point was smoothened by averaging the secondary chemical shifts of one residue immediately before and one residue after a given amino acid. The region corresponding to the β2- and the β2/β3-loop in each form is highlighted. The secondary structure of the protein is also included at the *top* of the figure. The data show remarkably similar secondary shift patterns (except for the β2-strand and the β2/β3-loop region) of the dimer and monomer forms of DLC8.

monomer equilibrium at neutral pH, and such equilibrium is pH-dependent.

When the pH of the DLC8bInsSG mutant was raised back from 3.0 to 7.0, the HSQC spectrum of the protein reversed to two sets of resonances corresponding to the monomer and dimer forms of the protein (data not shown). This finding indicates that the dimer-monomer equilibrium of DLC8bInsSG is reversible. This observation is in sharp contrast to that of the wild type protein, which is unable to re-form dimer by raising sample pH value. Hence we further conclude that the insertion of extra amino acid residues in the tight β1/β2 linker leads to a much more stable form of the monomeric DLC8b.

Conformation of DLC8bInsSG Both in Its Dimer and Monomer Forms—It was unexpected by us that DLC8bInsSG was unable to bind target proteins in neutral pH in the pull-down assay (Fig. 6). We further confirmed this observation by titrating ^{15}N-labeled DLC8bInsSG with a synthetic peptide comprising the DLC8-binding domain of the dynein intermediate chain (20, 21). The HSQC spectra of ^{15}N-labeled DLC8bInsSG at pH 7.0 in the presence and absence of the dynein intermediate

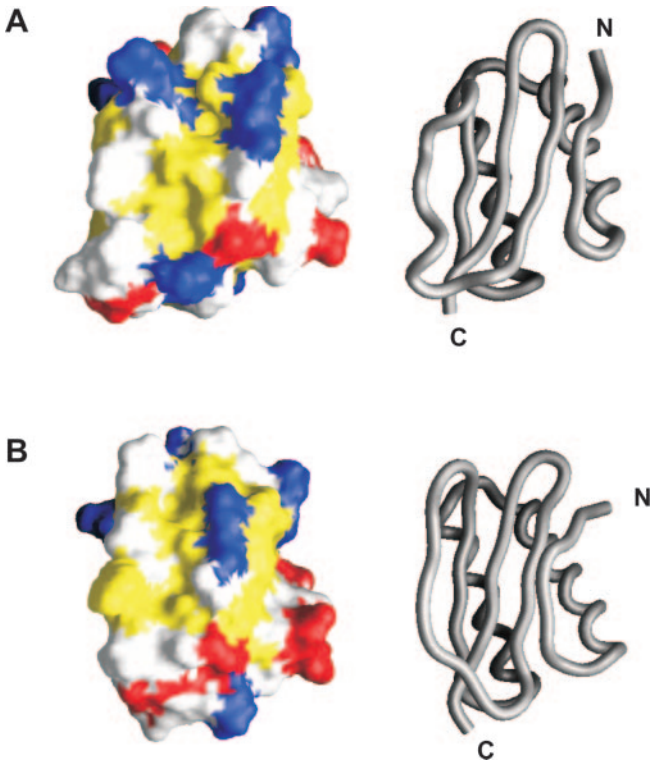

FIG. 5. **Surface representation of the DLC8b monomer (*A*) and a subunit of the DLC8a dimer (*B*).** The hydrophobic amino acid residues are shown in *yellow*, the positively charged residues are in *blue*, the negatively charged residues are in *red*, and the uncharged polar residues are in *gray*. The worm models shown at the *right* of each surface structure are used to indicate the orientations of the protein molecules.

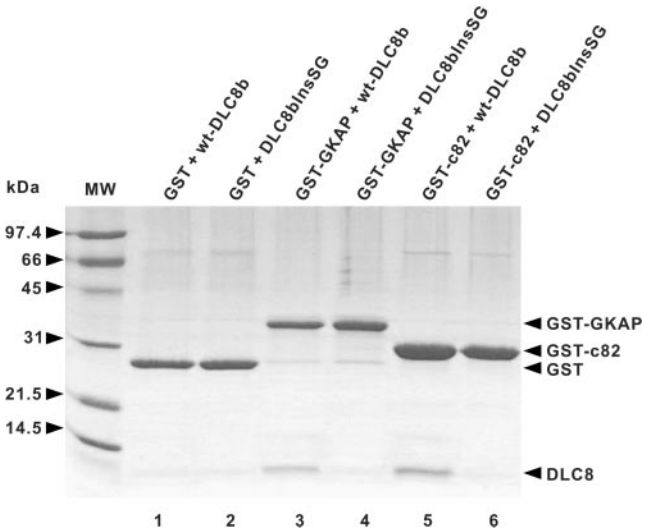

FIG. 6. **The DLC8InsSG mutant lacks target binding capability.** The figure shows the Coomassie Blue staining of SDS-polyacrylamide gel comparing target binding of DLC8b and DCL8bInsSG. The two DLC8 targets used in this assay were GKAP (17) and c82 (21). GKAP contains a "GIQV" DLC8-binding motif (20, 22), and c82 contains a "(K/R)XTQT" DLC8-binding motif (21). The DLC8-binding targets were fused to GST. *Lanes 1* and *2*, serving as control, show no nonspecific interaction between GST and two DLC8 proteins. *Lanes 3* and *4* compare the interaction of GST-GKAP with the wild type (*Lane 3*) and the mutant (*Lane 4*) DLC8b. *Lanes 5* and *6* compare the interaction of GST-c82 with the wild type (*Lane 5*) and the mutant (*Lane 6*) DLC8b. *wt*, wild type.

chain peptide are essentially identical (data not shown), further supporting that the mutant protein is unable to bind to target proteins in its dimer form. To understand the structural

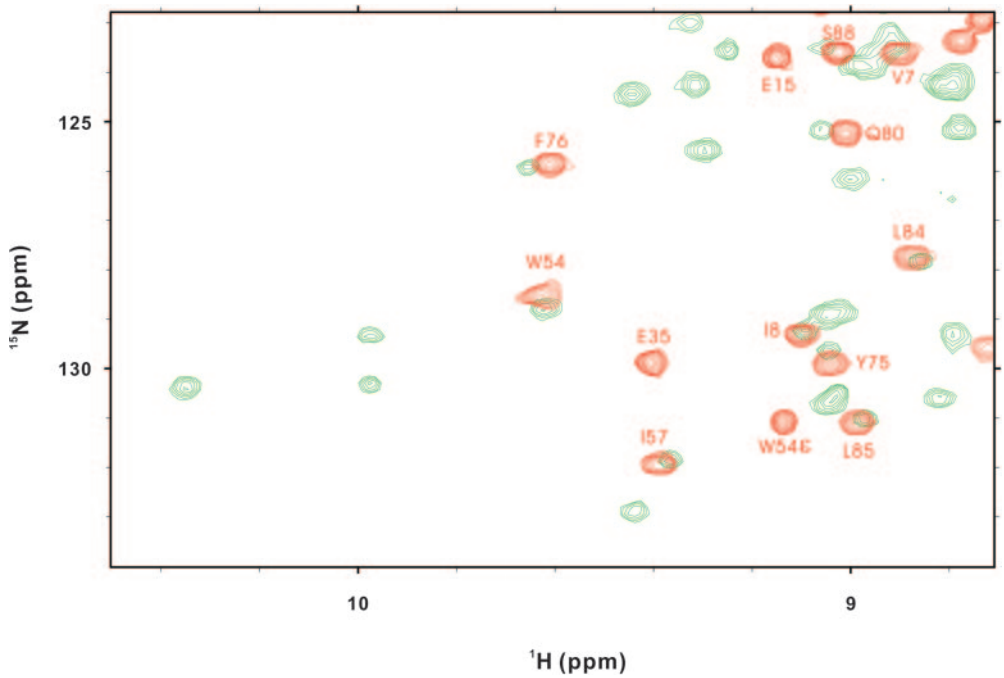

FIG. 7. **Dimer-monomer equilibrium of the DLC8bInsSG mutant.** The figure shows a superposition plot of the ^{1}H,^{15}N HSQC spectra of ^{15}N-labeled DLC8bInsSG at pH 7.0 (*green*) and pH 3.0 (*red*). The assignments of selected amino acid residues for the monomeric DLC8bInsSG are labeled. For clarity, only a selected region of each spectrum is plotted.

origin of the mutation-induced target binding disruption, we compared the ^{1}H,^{15}N HSQC spectrum of the DLC8bInsSG (recorded at pH 7.0) with the HSQC spectrum of the wild type DLC8b dimer (recorded at pH 7.0) (Fig. 8*A*). In comparing the two spectra, it is evident that major differences exist, indicating major conformational changes in the mutant protein. Since the chemical shift assignment of the wild type DLC8b is available and the peaks corresponding to the dimer form of DLC8bInsSG are also known (by removing the assigned monomer peaks), we were able to obtain mutation-induced conformational changes of the DLC8b dimer using the minimal chemical shift perturbation method (Fig. 8*B* and Ref. 41). The amino acid residues at the end of β1-strand, β1/β2 linker, and β2-loop of the mutant protein undergo the largest chemical shift changes. It is likely that the loss of target peptide binding is accompanied by the large conformational changes seen in the β2-strand of the mutant dimer as β2 acts as the receiving β-strand when the wild type DLC8 binds to its targets (19, 20). Our data further indicate that dimerization of the mutant is insufficient for the binding to its targets.

To understand the structural basis of the mutation-induced stabilization of the monomeric conformation, we determined the solution structure of DLC8bInsSG at pH 3.0 by NMR spectroscopy. The chemical shift assignment of the mutant at pH 3.0 (except the β1/β2 linker and the β2-loop region) could be largely transferred from that of the wild type protein at the same pH since very little chemical shift differences were observed between the two proteins (data not shown). The transferred chemical shift assignments were further confirmed by a three-dimensional ^{15}N NOESY spectrum. The chemical shifts of the residues in the β1/β2 linker and the β2-loop were then assigned by the three-dimensional ^{15}N NOESY spectrum. The structure of the mutant at pH 3.0 was determined by a total of 1,060 NOE restraints from a three-dimensional ^{15}N NOESY experiment, 66 hydrogen bonds, and 74 dihedral angle restraints. Due to the relatively low number of experimental restraints, the structure of the DLC8bInsSG monomer was determined at a medium precision (Fig. 9). Nevertheless the structure allowed us to observe mutation-induced conformational changes of the DLC8bInsSG monomer. Except for the regions at the end of β1 and the β1/β2 linker, the structure of the DLC8bInsSG monomer is essentially identical to that of the DLC8b monomer (Fig. 9*B*). Insertion of two residues in the β1/β2 linker appears to release the tight restraint in the wild type protein. The β1-strand of the mutant extends one residue further and has the same length as the β1-strand in the dimer of the wild type protein. In addition, the mutation causes the β2-loop to become a more stable α-helix. It is likely that the more stable conformation of the DLC8bInsSG monomer is afforded by the energetic gains realized through the conformational stabilization in the above two regions.

DISCUSSION

The Domain-swapped Dimer Is Required for DLC8 to Bind to Its Targets—It is well established that the functional unit of DLC8 is in its dimer form (10, 19, 20). The β2-strand in each subunit swaps with each other to form a domain-swapped dimer assembly. In addition to the intersubunit backbone hydrogen bonds between the β1-strand and the swapped β2-strand, the dimer interface also involves extensive hydrophobic interactions formed between the two β-sheets. At neutral pH, DLC8 adopts a stable dimer conformation (19, 20, 40, 42). However, DLC8 gradually dissociates into a monomer upon lowering the pH value of the protein solution (Ref. 40 and this study). The high energy barrier between the β2-loop conformation in the monomer and the β2-strand structure in the dimer might be responsible for the irreversible pH-dependent dimer-to-monomer dissociation of DLC8. However, we do not have definitive experimental evidence to prove this hypothesis at this stage. Earlier circular dichroism and current NMR studies showed that the protein adopts a stably folded monomer at pH 3.0 (40). The dimer-to-monomer transition is accompanied by significant conformational changes of the protein. Specifically the β2-strand seen in the dimer form of the protein no longer adopts a β-strand structure in its monomer form. Instead it becomes a nascent α-helix structure. Such a conformational change appears to be necessary for the stable folding of DLC8 monomer in solution. Protein binding experiments using NMR

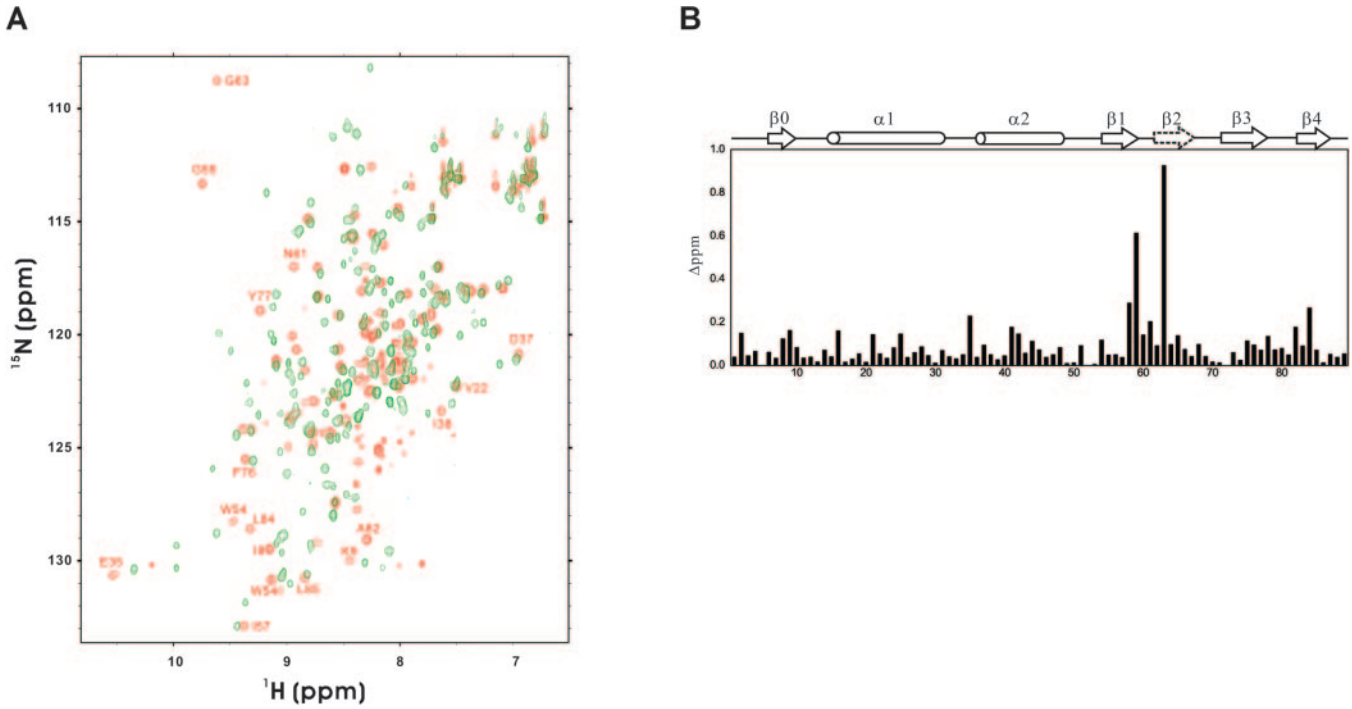

FIG. 8. **The DLC8bInsSG dimer adopts a conformation different from that of the wild type DLC8b dimer.** *A*, superposition of the ^{1}H,^{15}N HSQC spectra of ^{15}N-labeled DLC8b (*red*) and DLC8bInsSG (*green*) at pH 7.0. At this pH, the wild type DLC8b exists as pure dimer, and DLC8bInsSG exists as dimer-monomer equilibrium. The peaks corresponding to the monomeric protein can be assigned by referring to the HSQC spectrum of the protein at pH 3.0. *B*, the combined ^{1}H and ^{15}N chemical shift differences as a function of amino acid residue between the DLC8b dimer and the DLC8bInsSG dimer using the minimal shift perturbation approach. The combined shift difference of each residue is defined as $\Delta\text{ppm} = \sqrt{(\Delta\delta_{HN})^2 + (\Delta\delta_N \times \alpha_N)^2}$. The scaling factor ($\alpha_N$) used to normalize the ^{1}H and ^{15}N chemical shifts is 0.17. The set of the peaks corresponding to the monomeric DLC8bInsSG was removed in the process of computing the minimal chemical shift change for each residue. The secondary structure of the DLC8 dimer is included at the *top* of the figure.

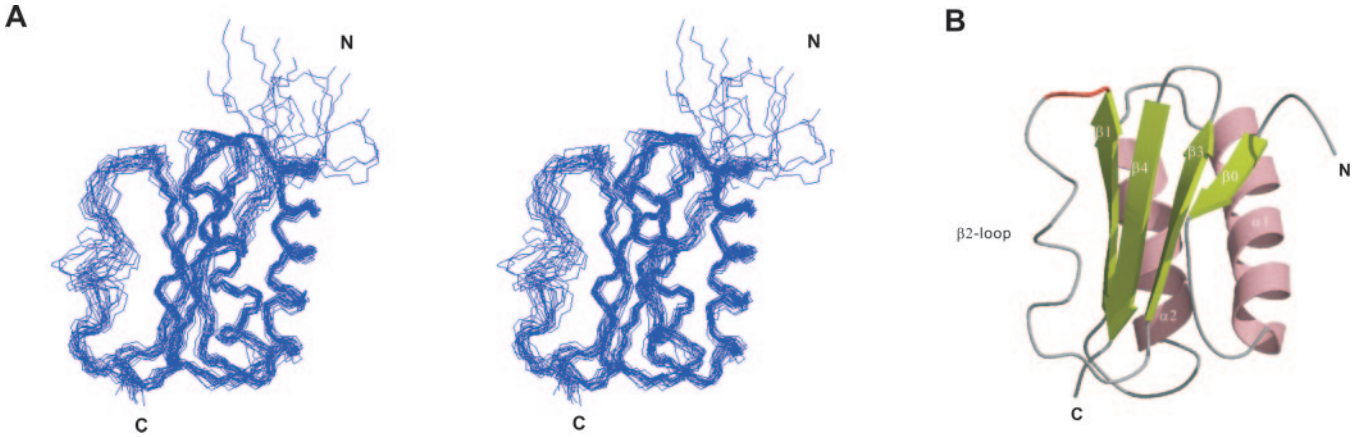

FIG. 9. **Three-dimensional structure of the DLC8bInsSG monomer.** *A*, stereoview showing the best fit superposition of the backbone atoms (N, C_α, and C′) of the final 20 structures of the DLC8bInsSG monomer. The structures are superimposed against the averaged structure using the secondary structured regions. *B*, ribbon diagram representation of the DLC8bInsSG monomer. The inserted residues in the β1/β2-loop are highlighted using *red* color. The secondary structure of the protein is also labeled.

and biochemical approaches showed that the monomeric form of DLC8 cannot interact with its target proteins. The structure of DLC8b monomer solved in this work provides a clear explanation for the functional loss that occurs as a result of protein dissociation. Each peptide-binding channel in the DLC8 dimer is formed by β0, β2, and β3 of one subunit and the α2-helix of the other subunit. The β2-strand at the base of each target-binding channel acts as the receiving β-strand to form anti-parallel β-sheet with target peptides (19, 20). The melting of the β2-strand as well as the departure of the α2-helix from the neighboring subunit that occurs upon dimer dissociation would certainly destroy the target-binding channel of the protein (Fig. 3).

We originally hypothesized that the melting of the β2-strand upon the dissociation of the dimer might result from the conformational restraint of the short β1/β2-loop. If this hypothesis were true, insertion of flexible amino acid residues in this region (*e.g.* Gly and Ser used in this study) would be expected to alleviate the conformational restraint of the loop. Moreover the resultant mutant monomer might be predicted to adopt a conformation similar to that seen in the wild type dimer with the exception that the β2-strand might fold back to form anti-parallel β-sheet with the β1-strand within the same subunit (*i.e.* a closed monomer conformation). Our data showed that the insertion mutation indeed stabilized the monomer conformation. As a matter of fact, we can detect a high population of the monomer even at neutral pH (Fig. 7). In contrast to our original expectation, DLC8bInsSG adopts a conformation very similar

to the wild type monomer with the β2-loop protruding out of the main β-sheet (Fig. 9). Consistent with this structural finding, the mutant monomer was unable to bind to target proteins.

To our surprise, the insertion mutant in its dimer form was also unable to bind target proteins (Fig. 6). NMR studies showed that the amino acid residues at the end of β1-strand, β1/β2 linker, and β2-loop (the β2-strand in the wild type dimer) adopt a very different conformation in the mutant dimer with respect to the wild type dimer. Due to the dimer-monomer equilibrium at neutral pH, we were unable to obtain a detailed picture of the dimer structure of the mutant. Nevertheless we predict that the β2-loop is not likely going to form a β-strand structure in the mutant dimer, and therefore the mutant dimer is formed without undergoing the β2-mediated domain swapping observed in the wild type dimer. This prediction is primarily based on the large chemical shift differences between the mutant and the wild type protein in the regions of the β2-strand and the β1/β2-loop. The definitive answer to this point requires the three-dimensional structure of the mutant dimer. Taken together, the experimental evidence suggests that the domain swapping-mediated dimer assembly is a mandatory requirement for the biological function of DLC8. Any change leading to the alteration of the domain swapping and dimer assembly in the native protein is likely to have a disastrous functional impact on the protein. Consistent with this prediction is the fact that the amino acid sequences of DLC8 orthologs in the β1 and β2 regions are almost completely conserved throughout evolution.

The Non-classical Domain Swapping in DLC8—In the classical definition of three-dimensional domain swapping, a protein is considered to be assembled via *bona fide* domain swapping as long as both the domain-swapped dimer and monomer conformations are stable, and the monomer has a closed conformation (for reviews, see Refs. 43–45). In this sense, the assembly of the DLC8 dimer can be considered as a case of three-dimensional domain swapping. However, the structure of the DLC8b monomer deviates from the conventional closed conformation. If the DLC8 monomer were to adopt a *bona fide* closed conformation, the β2-loop should fold back to form antiparallel β-sheet with β1 within the same subunit (as the β2-strand from another subunit does in the dimer). Instead the β2-loop adopts a nascent α-helix structure that protrudes from the main β-sheet (*i.e.* a distorted "open" conformation) in the monomer (Fig. 3). Furthermore the DLC8 dimer assembly is unusual in the context of three-dimensional domain swapping given that the overwhelming majority of domain swappings occur either at the N or the C termini of proteins (43–45). The region responsible for the domain swapping in DLC8 is located near the center of the protein (the β2-strand). Thus, the DLC8 dimer should be classified as a non-conventional case of three-dimensional domain swapping.

In summary, we characterized the pH-dependent dimer-monomer equilibrium of DLC8 in great detail. The structure of the monomeric DLC8b shows a clever solution for the stable folding of the protein by adjusting the conformation of the orphan β2-strand resulting from dimer dissociation. Structural and biochemical studies showed that the β2-strand-mediated domain swapping and dimer assembly are obligatory for the function of the protein. The tight β1/β2 linker plays an important role for the proper dimer assembly of the DLC8.

Acknowledgment—We thank Dr. David Miller-Martini for critical reading of the manuscript.

REFERENCES

1. Holzbaur, E. L., and Vallee, R. B. (1994) *Annu. Rev. Cell Biol.* **10,** 339–372
2. Vallee, R. B., and Sheetz, M. P. (1996) *Science* **271,** 1539–1544
3. King, S. M. (2000) *Biochim. Biophys. Acta* **1496,** 60–75
4. Vale, R. D. (2003) *Cell* **112,** 467–480
5. Gill, S. R., Cleveland, D. W., and Schroer, T. A. (1994) *Mol. Biol. Cell* **5,** 645–654
6. Hughes, S. M., Vaughan, K. T., Herskovits, J. S., and Vallee, R. B. (1995) *J. Cell Sci.* **108,** 17–24
7. Piperno, G., and Luck, D. J. (1979) *J. Biol. Chem.* **254,** 3084–3090
8. King, S. M., and Patel-King, R. S. (1995) *J. Biol. Chem.* **270,** 11445–11452
9. King, S. M., Barbarese, E., Dillman, J. F., III, Patel-King, R. S., Carson, J. H., and Pfister, K. K. (1996) *J. Biol. Chem.* **271,** 19358–19366
10. Benashski, S. E., Harrison, A., Patel-King, R. S., and King, S. M. (1997) *J. Biol. Chem.* **272,** 20929–20935
11. Espindola, F. S., Suter, D. M., Partata, L. B., Cao, T., Wolenski, J. S., Cheney, R. E., King, S. M., and Mooseker, M. S. (2000) *Cell Motil. Cytoskelet.* **47,** 269–281
12. Jaffrey, S. R., and Snyder, S. H. (1996) *Science* **274,** 774–777
13. Fan, J. S., Zhang, Q., Li, M., Tochio, H., Yamazaki, T., Shimizu, M., and Zhang, M. (1998) *J. Biol. Chem.* **273,** 33472–33481
14. Puthalakath, H., Huang, D. C., O'Reilly, L. A., King, S. M., and Strasser, A. (1999) *Mol. Cell* **3,** 287–296
15. Puthalakath, H., Villunger, A., O'Reilly, L. A., Beaumont, J. G., Coultas, L., Cheney, R. E., Huang, D. C., and Strasser, A. (2001) *Science* **293,** 1829–1832
16. Schnorrer, F., Bohmann, K., and Nusslein-Volhard, C. (2000) *Nat. Cell Biol.* **2,** 185–190
17. Naisbitt, S., Valtschanoff, J., Allison, D. W., Sala, C., Kim, E., Craig, A. M., Weinberg, R. J., and Sheng, M. (2000) *J. Neurosci.* **20,** 4524–4534
18. Fuhrmann, J. C., Kins, S., Rostaing, P., El Far, O., Kirsch, J., Sheng, M., Triller, A., Betz, H., and Kneussel, M. (2002) *J. Neurosci.* **22,** 5393–5402
19. Liang, J., Jaffrey, S. R., Guo, W., Snyder, S. H., and Clardy, J. (1999) *Nat. Struct. Biol.* **6,** 735–740
20. Fan, J. S., Zhang, Q., Tochio, H., Li, M., and Zhang, M. (2001) *J. Mol. Biol.* **306,** 97–108
21. Lo, K. W., Naisbitt, S., Fan, J. S., Sheng, M., and Zhang, M. (2001) *J. Biol. Chem.* **276,** 14059–14066
22. Rodriguez-Crespo, I., Yelamos, B., Roncal, F., Albar, J. P., Ortiz de Montellano, P. R., and Gavilanes, F. (2001) *FEBS Lett.* **503,** 135–141
23. Phillis, R., Statton, D., Caruccio, P., and Murphey, R. K. (1996) *Development* **122,** 2955–2963
24. Dick, T., Ray, K., Salz, H. K., and Chia, W. (1996) *Mol. Cell. Biol.* **16,** 1966–1977
25. Beckwith, S. M., Roghi, C. H., Liu, B., and Ronald Morris, N. (1998) *J. Cell Biol.* **143,** 1239–1247
26. Tochio, H., Ohki, S., Zhang, Q., Li, M., and Zhang, M. (1998) *Nat. Struct. Biol.* **5,** 965–969
27. Delaglio, F., Grzesiek, S., Vuister, G. W., Zhu, G., Pfeifer, J., and Bax, A. (1995) *J. Biomol. NMR* **6,** 277–293
28. Garrett, D. S., Powers, R., Gronenborn, A. M., and Clore, G. M. (1991) *J. Magn. Reson.* **95,** 214–220
29. Bax, A., and Grzesiek, S. (1993) *Acc. Chem. Res.* **26,** 131–138
30. Kay, L. E., and Gardner, K. H. (1997) *Curr. Opin. Struct. Biol.* **7,** 722–731
31. Clore, G. M., and Gronenborn, A. M. (1997) *Nat. Struct. Biol.* **4,** (suppl.) 849–853
32. Wüthrich, K. (1986) *NMR of Proteins and Nucleic Acids*, John Wiley, New York
33. Cornilescu, G., Delaglio, F., and Bax, A. (1999) *J. Biomol. NMR* **13,** 289–302
34. Brunger, A. T., Adams, P. D., Clore, G. M., DeLano, W. L., Gros, P., Grosse-Kunstleve, R. W., Jiang, J. S., Kuszewski, J., Nilges, M., Pannu, N. S., Read, R. J., Rice, L. M., Simonson, T., and Warren, G. L. (1998) *Acta Crystallogr. Sect. D Biol. Crystallogr.* **54,** 905–921
35. Laskowski, R. A., Rullmannn, J. A., MacArthur, M. W., Kaptein, R., and Thornton, J. M. (1996) *J. Biomol. NMR* **8,** 477–486
36. Koradi, R., Billeter, M., and Wuthrich, K. (1996) *J. Mol. Graph.* **14,** 51–55
37. Kraulis, P. J. (1991) *J. Appl. Crystallogr.* **24,** 946–950
38. Merritt, E., and Murphy, M. (1994) *Acta Crystallogr. Sect. D Biol. Crystallogr.* **50**, 869–873
39. Nicholls, A. (1992) *GRASP: Graphical Representation and Analysis of Surface Properties*, Columbia University, New York
40. Barbar, E., Kleinman, B., Imhoff, D., Li, M., Hays, T. S., and Hare, M. (2001) *Biochemistry* **40,** 1596–1605
41. Farmer, B. T., II, Constantine, K. L., Goldfarb, V., Friedrichs, M. S., Wittekind, M., Yanchunas, J., Jr., Robertson, J. G., and Mueller, L. (1996) *Nat. Struct. Biol.* **3,** 995–997
42. Fan, J. S., Zhang, Q., Tochio, H., and Zhang, M. (2002) *J. Biomol. NMR* **23,** 103–114
43. Bennett, M. J., Schlunegger, M. P., and Eisenberg, D. (1995) *Protein Sci.* **4,** 2455–2468
44. Liu, Y., and Eisenberg, D. (2002) *Protein Sci.* **11,** 1285–1299
45. Newcomer, M. E. (2002) *Curr. Opin. Struct. Biol.* **12,** 48–53